OBTAINING LIMITED DIFFRACTION BEAMS WITH THE WAVELET TRANSFORM†

Hehong Zou, Jian-yu Lu and *James F. Greenleaf*
Biodynamics Research Unit, Department of Physiology and Biophysics,
Mayo Clinic and Foundation, Rochester, MN 55905

ABSTRACT

Generating limited diffraction (or nondiffracting theoretically) beams involves deriving special solutions to a homogeneous wave equation. Previous results have been derived by the Fourier [1] and Laplace [6] transforms. In this paper, we use the wavelet transform to obtain a novel nondiffracting solution. It can be shown that this new solution is equivalent to the second derivative of Lu-Greenleaf's zero-th order X wave [6] or the first derivative of Donnelly's Localized wave [1]. The advantage of the wavelet beams is their localization property, that is, they have smaller sidelobes compared with the previous results. The magnitude decays as $1/r^3$ along the lateral (r) direction. Although the slowest decay is still $1/\sqrt{r}$ asymptotically, the sidelobes are reduced to about half those of the broadband X wave [6]. We also show that this new nondiffracting beam can be realized as a limited diffraction beam with finite energy and finite aperture ultrasound transducers.

I. INTRODUCTION

The recently explored limited diffraction beams (obtained from unique nondiffracting solutions to the homogeneous wave equation) possess some important desirable features and could become an alternative ultrasonic beam forming technique. Unlike the conventional focus beams, which usually focus in fixed or varying points, such a beam focuses all the way along the wave propagation direction. It has been shown previously that this new beam has almost constant lateral and axial beam profiles within a large depth of field.

Obtaining limited diffraction beams involves deriving special nondiffracting solutions to the free space (homogeneous) wave equation. Previous nondiffracting solutions have been derived by the Laplace [1] and Fourier [6] transforms. In this paper, we apply the wavelet theory developed by Kaiser [3,4] to obtaining a novel solution to the wave equation. It can be shown in [8] that this new solution is equivalent to the second derivative of Lu-Greenleaf's zero-th order X wave or the first derivative of Donnelly's Localized wave. The advantage of the wavelet beams is their localization property, that is, they have smaller sidelobes compared with the previous results. The magnitude decays as $1/r^3$ along the lateral (r) direction. Although the slowest decay in the X branch is still $1/\sqrt{r}$ asymptotically, the sidelobes are reduced to about half those of the X wave solution. We also show by the computer simulations that this new nondiffracting wavelet can be realized as a limited diffraction beam with finite energy and finite aperture ultrasound transducers.

This paper serves to summarize the results derived in [9]. In the next section, the basic idea of free space wave equation and localized wavelet solutions are briefly discussed. We also show that such a solution can be extended to obtain a nondiffracting solution. The main properties of this wavelet beam will be highlighted. We then demonstrate in section III that this special wavelet can be realized approximately by finite aperture ultrasonic transducers. Conclusion will be made finally in section V.

II. WAVELETS AND WAVE EQUATION

It is well known that the ultrasonic wave propagating in a homogeneous medium is governed by the following wave equation

$$\left[\frac{\partial^2}{\partial x^2}+\frac{\partial^2}{\partial y^2}+\frac{\partial^2}{\partial z^2}-\frac{1}{c^2}\frac{\partial^2}{\partial t^2}\right]\phi(x,y,z,t)=0, \quad (1)$$

where $\phi(x,y,z,t)$ denotes the acoustical pressure at the three dimensional space (x,y,z) and time t, and c is the speed of sound in the medium. To study the wave propagation, it is necessary to derive a special solution to the aforementioned wave equation. For instance, the previous nondiffacting and localized wave solutions are derived by the Laplace [6] and Fourier [1] transforms on (1). Alternatively, the wavelet theory developed by Kaiser in [3,4] can also be used to obtain a localized wavelet solution to this wave equation. Specifically, the wavelet transform solution has a closed form as,

$$\phi(x,y,z,t)=\frac{3(\alpha_0+jct)^2-\rho^2}{\left[(\alpha_0+jct)^2+\rho^2\right]^3} \quad (2)$$

where α_0 is a real constant, $j=\sqrt{-1}$, and $\rho=\sqrt{x^2+y^2+z^2}$.

Note that the above solution specifies a localized wave. It decays in the cubic order along the directions of x, y, z and t. In other words, the wave governed by (2) does not travel in any spatial direction. However, our goal here is

†This work was supported in part by grants CA54212 and CA43920 from the National Institutes of Health.

1051-0117/93/0000-1087 $4.00 © 1993 IEEE

to construct a wave (or beam) which can propagate in the z direction as time t and does not spread when propagating. That is, we are seeking a solution such that the term $z - \gamma t$ appears together in the closed form as otherwise obtained previously, where γ is a real constant related to speed of sound c. To achieve this goal we first solve the following equation

$$\left[\frac{\partial^2}{\partial x^2} + \frac{\partial^2}{\partial y^2} - \frac{1}{c^2}\frac{\partial^2}{\partial t^2}\right]\phi(x,y,t) = 0, \tag{3}$$

where $\phi(x,y,t)$ denotes the acoustical pressure at the two dimensional space (x,y) and time t. Following the same wavelet theory developed in [3,4] and extended in [9], one can get the following solution,

$$\phi(x,y,t) = \frac{2(\alpha_0 + jct)^2 - r^2}{\left[(\alpha_0 + jct)^2 + r^2\right]^{\frac{5}{2}}} \tag{4}$$

where $r = \sqrt{x^2 + y^2}$. By interchanging variables

$$\begin{aligned} r\sin\zeta &\rightarrowtail r, \\ ct - z\cos\zeta &\rightarrowtail ct, \end{aligned} \tag{5}$$

where ζ is a real constant, into the above solution, it is easy to obtain a new solution,

$$\phi(\vec{r},z,t) = \frac{2(\alpha_0 + j(z\cos\zeta - ct))^2 - (r\sin\zeta)^2}{\left[(\alpha_0 + j(z\cos\zeta - ct))^2 + (r\sin\zeta)^2\right]^{\frac{5}{2}}}. \tag{6}$$

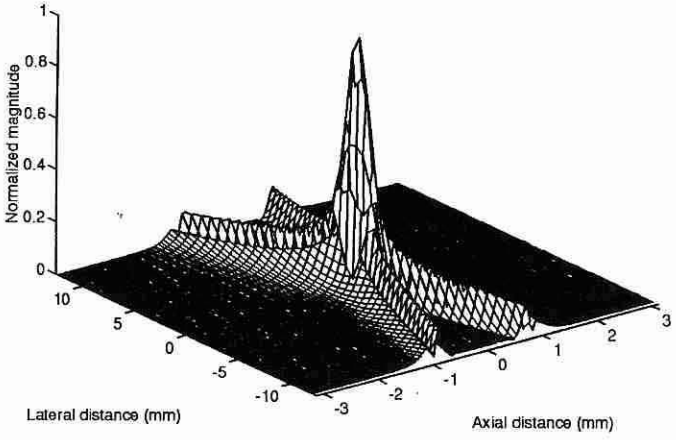

Figure 1. Real part of wavelet (6) at $t = 0$ for parameters $\zeta = 4^o$, $\alpha_0 = 0.2$ (mm), and $c = 1500$ (m/s).

This is a novel nondiffracting solution called wavelet. Figure 1 shows the real part of this wavelet at $t = 0$ which also resembles an X shape. For any other time t, the center wave moves to $z = \frac{ct}{\cos\zeta}$ while it still maintains the same shape according to (6). That is, the wavelet propagates in the z (axial) direction with the phase speed $\frac{c}{\cos\zeta}$ without spreading or diffracting. The advantage of the wavelet beams is their localization property, that is, they have smaller sidelobes compared with the previous results. The magnitude decays as $1/r^3$ along the lateral (r) direction. Although the slowest decay is still $1/\sqrt{r}$ asymptotically, the sidelobes are reduced to about half those of the broadband X wave [6].

It has also been shown in [9] that Fourier transform (with respect to time t) of (6) has the following closed form,

$$\Phi(\vec{r},z,\omega) = \tfrac{2\pi}{c}\left(\tfrac{\omega}{c}\right)^2 J_0\left(\tfrac{\omega}{c}r\sin\zeta\right)\mu\left(\tfrac{\omega}{c}\right)e^{-[\alpha_0 - jz\cos\zeta]\frac{\omega}{c}} \tag{7}$$

where $J_i(\bullet)$ denotes the ith order Bessel function of the first kind, $\Gamma(\bullet)$ is the Gamma function, and $\mu(x)$ is defined as the following step function,

$$\mu(x) = \begin{cases} 1 & \text{for } x \geq 0 \\ 0 & \text{otherwise} \end{cases}. \tag{8}$$

It is pointed out in [8] that this wavelet solution is the first derivative of Donnally's localized wave and the second derivative of Lu-Greenleaf's X wave. Figures 2 (a) and (b) show the axial beam profile $\phi(z\cos\zeta - ct)|_{\vec{r}=0}$ and its Fourier transform $\Phi(\omega)|_{\vec{r}=0}$. One can see from these two figures that $\phi(z\cos\zeta - ct)|_{\vec{r}=0}$ is essentially the Mexican Hat wavelet with two vanishing moments (that is, the Fourier transform in (7) has a zero of order two at $\omega = 0$) [9]. Figure 2 (c) shows the lateral beam profile of the wavelet, where $z = \frac{ct}{\cos\zeta}$, which is a smooth function. We also draw in Figure 2 (d) the wavelet beam profile along the X branch (the slowest decay direction). The beam decays quickly around its center and slowly when r further increases. Hence, the wavelet, like other limited diffraction beams, has relatively higher sidelobes than the conventional focused beams at their focal range.

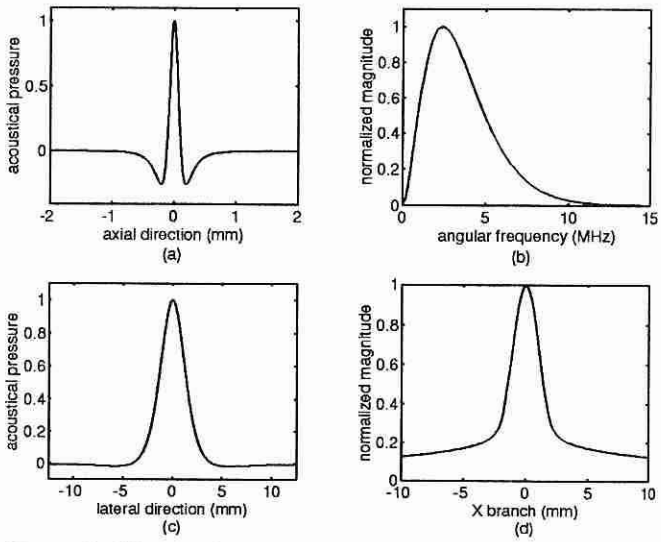

Figure 2. The wavelet beam profile (real part of (6)). (a) axial beam profile, (b) Fourier transform of (a), (c) lateral beam profile, (d) beam profiles along the X branch (i.e., the slowest decay direction).

To summarize so far, the wavelet solution to the scalar wave equation is a nondiffracting solution. This type of

beam propagates along the axial direction as a group of wavelets having two vanishing moments without spreading or diffracting. To maintain its non-diffraction nature, a relatively strong X branch which decays in order of $\frac{1}{\sqrt{r}}$ must exist to continuously support the center wave. This is probably the reason why the unique X like beam can travel to infinite distance without changing its spatial shape.

III. FINITE APERTURE SIMULATIONS

While the wavelet solution (6) to the free space wave equation (1) represents a nondiffracting beam, its exact realization is rather difficult due to two reasons. One is that the practical ultrasound transducers may have difficulty generating the exactly required waveform (6). Obtaining the exact waveform by deriving the transducer transfer function is not practical because the transfer function varies for different transducers. Another difficulty results from the fact that practical transducers always have finite aperture size. In this section, we discuss the approximate realization of the nondiffracting wave that results in the so called limited diffraction wavelet. In this case, the wavelet (6) can travel to a large distance (thus large depth of field) while maintaining approximately the constant beam profiles.

We begin by assuming that the wavelet is radiated by an ultrasonic source transducer located at the plane $z = 0$. Without loss of generality, one can assume that the radiator is circular and has a finite diameter D. In particular, the Fourier transform of ϕ, the source beam profile, can be written as,

$$E(\vec{r},\omega) = \Phi(\vec{r}, z=0, \omega) = \begin{cases} \frac{2\pi}{c}\left(\frac{\omega}{c}\right)^2 J_0\left(\frac{\omega}{c} r \sin\zeta\right)\mu\left(\frac{\omega}{c}\right)e^{-\alpha_0\frac{\omega}{c}} & \text{if } r \le \frac{D}{2} \\ o & \text{otherwise} \end{cases}. \quad (9)$$

We now use this source to simulate the waves radiated into an isotropic homogeneous medium. According to [2], the Fourier transform of an acoustical wave at any spatial location $(\vec{r}, z)$ for any frequency ω can be calculated by the following Raleigh-Sommerfeld diffraction formula,

$$\Phi_{\vec{r}}(\vec{r},k) = \frac{1}{j\lambda}\int_0^{2\pi}\int_0^{\frac{D}{2}} d\theta' r' dr' E(\vec{r},k)\frac{e^{jkr_{01}}}{r_{01}^2} z + \frac{1}{2\pi}\int_0^{2\pi}\int_0^{\frac{D}{2}} d\theta' r' dr' E(\vec{r},k)\frac{e^{jkr_{01}}}{r_{01}^3} z, \quad (10)$$

where $k = \frac{\omega}{c}$ denotes the wave number. The first and second terms of the right side in (10) represent the low and high frequency contributions, respectively.

The transmitted wave received at any point in the field can then be obtained through the inverse Fourier transform of (10), that is,

$$\phi_z(\vec{r},t) = \mathcal{F}^{-1}[\Phi_z(\vec{r},k)]. \quad (11)$$

Figures 3 (a)-(d) illustrate the wavelet beam profiles at depth $z = 30, 60, 90, 150$ (mm), respectively. The parameters used in this simulation is the same as in the previous figures and $D = 25$ (mm). The peaked value of the produced wavelet along the propagation direction is also shown in figure 3 (e). It is seen from the figures that the rear X branch is gradually weakened as the wavelet propagates deeper into the field. Once the rear X branch disappears completely, the beam will diffract beyond the depth of field $Z_{max} = 178$ (mm) [6,8,9].

Next, we consider the influence of the practical ultrasound transducer. As shown in the previous simulations and experiments [6,7,9], the firing excitation of each transducer in this case now becomes,

$$E_b(\vec{r},\omega) = E(\vec{r},\omega)B(\omega) = \begin{cases} \frac{2\pi}{c}\left(\frac{\omega}{c}\right)^2 J_0\left(\frac{\omega}{c} r \sin\zeta\right)\mu\left(\frac{\omega}{c}\right)B(\omega)e^{-\alpha_0\frac{\omega}{c}} & \text{if } r \le \frac{D}{2} \\ 0 & \text{otherwise} \end{cases}, \quad (12)$$

where $B(\omega)$ denotes the transducer transfer function, which can usually be modeled as a Blackman window [6]. Equations (10)—(12) infer that the constructed acoustical field can be calculated simply by (11) convoluted by $b(t)$ (the inverse Fourier transform of $B(\omega)$). The resulting beam profiles can be found in [9].

IV. CONCLUSION

We have applied the wavelet theory developed in [3,4,9] to obtaining a special solution to the free space scalar wave equation. The wave governed by this solution is a nondiffracting beam. Even with a practical ultrasonic transducer of finite energy and finite aperture, a good approximation is achieved in that the wavelet has almost constant lateral and axial profiles and large depth of field. Comparing our new result with the previous ones, it seems that we have achieved the limit of the nondiffracting beams in which the X branch should have sufficient energy to maintain the nondiffracting nature of the beam. As we also have mentioned, practical transducers have system transfer functions similar to figure 2 (b). This may explain why X wave have smaller side lobes when realized by practical ultrasonic transducers.

Finally, it is worth mentioning here that the recently developed wavelet theory is an important tool for the signal processing. Not only can it give a closed form wavelet solution, but it also has advantages in postprocessing the medical images obtained. An interesting example is given in [5] in which Daubechies' orthonormal wavelets were proposed in the ultrasound imaging system.

V. ACKNOWLEDGMENTS

The authors appreciate the secretarial assistance of Elaine C. Quarve.

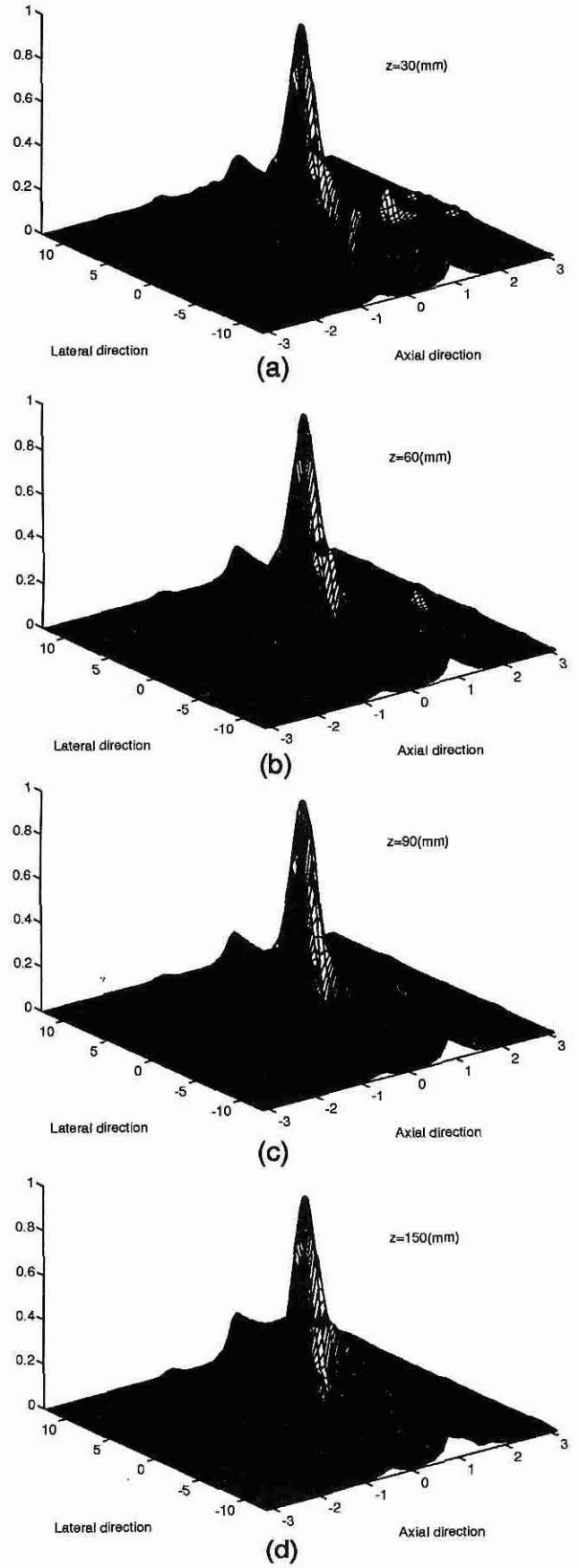

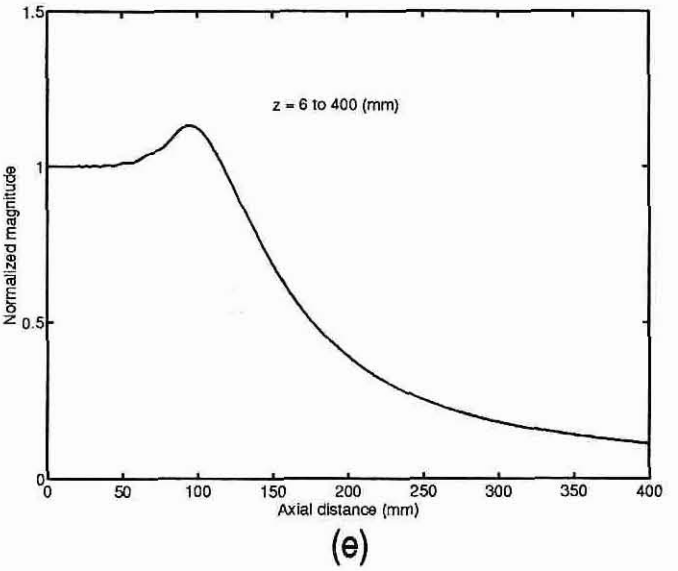

Figure 3. (a)-(d) the wavelet beam profiles at different depth ($z = 30, 60, 90, 150$ (mm)) when produced with an ultrasound transducer with diameter $D = 25$ (mm), (e) the peaked value of the produced wavelet along the wave propagation (z) direction.

REFERENCES

[1]. R. Donnelly, D. Power, G. Templeman, and A. Whalen: "Graphical simulation of superluminal acoustic localized wave pulses." to appear IEEE Trans. Ultrason Ferroelec., Freq. Contr..

[2]. J. W. Goodman, *Introduction to Fourier Optics*. New York, NY: McGraw-Hill, 1968, chs. 2-4.

[3]. G. Kaiser, "Wavelet electrodynamics", Physics letters A, vol. 168, pp. 28-34, 1992.

[4]. G. Kaiser and R. F. Streater, "Windowed radon transforms, analytic signals and the wave equation",*Wavelets—a tutorial in theory and applications*. C. K. Cui, ed. Academic Press, New York, 1992.

[5]. J. H. Lether, "An imaging device that uses the wavelet transformation as the image reconstruction algorithm", Int'l J. of Imaging Sys. and Tech., pp. 98-108, 1992.

[6]. Jian-yu Lu, and J. F. Greenleaf, "Nondiffracting X waves—exact solutions to free-space scalar wave equation and their finite aperture realizations," IEEE Trans. UFFC 39(1):19-31, Jan., 1992.

[7]. Jian-yu Lu and J. F. Greenleaf, "Experimental verification of nondiffracting X waves," IEEE Trans. UFFC 39(3):441-446, May, 1992.

[8]. Jian-yu Lu, H. Zou and J. F. Greenleaf, "Biomedical ultrasound beam forming," to appear Ultrasound in Medicine and Biology.

[9]. H. Zou, Jian-yu Lu and J. F. Greenleaf, "A limited diffraction beam obtained by wavelet theory," to be submited to IEEE Trans. UFFC, Nov. 1993.